Norwegian Meteorological Institute
met.no

met.no report

Report no. 1/2011
Oceanography
ISSN: 1503-8025
Oslo, February 9, 2011

KARBIAC Phase II b Final Report: Description of model and discussion of model results

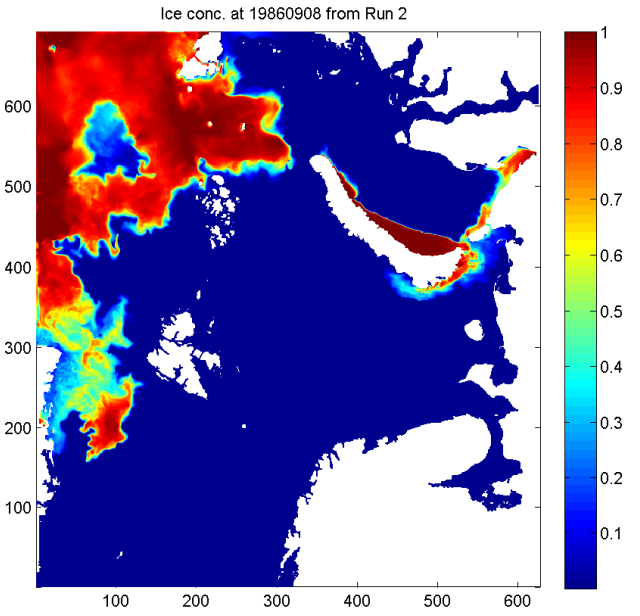

INSTITUTE OF MARINE RESEARCH
HAVFORSKNINGSINSTITUTTET

Norwegian Meteorological Institute
met.no

Norwegian Meteorological Institute
met.no

report

Number	Subject	Date	Classification	ISSN
1/2011	Oceanography	February 9, 2011	☒ Open ☐ Restricted ☐ Confidential	1503-8025

Title

KARBIAC Phase II b Final Report: Description of model and discussion of model results

Authors

Lars Petter Røed[1] and W. Paul Budgell[2]

Client(s)	Client reference
Statoil (Børge Kvingedal)	Contract No. 4501790631

Abstract

We report on the work performed by the Norwegian Meteorological Institute and the Institute of Marine Research regarding Phase 2b of the Joint Industry Project KARBIAC (KARa and Barents Seas Ice And Current). The work consists of (1) testing changes and corrections to the ROMS version used in the earlier Phase 2, (2) deciding on a new version for Phase 2b, (3) performing two new hindcasts using (a) ERA40 reanalysis and (b) the higher resolution archived HIRLAM 10 km as atmospheric forcing, (4) delivering agreed upon model results and (5) delivering a technical report. The tests in item 1 include ten new short (one to two months) tidal simulations, and three full runs for three years. The new hindcasts are each one year long. We did not encounter any major technical problems during the test and hindcast runs. Time series of water level (tides and storm surges), horizontal current components, temperature and salinity at preselected locations were extracted. Also ice concentration fields were extracted. The model's skill in reproducing the observations is assessed by a third party.

Keywords

Physical Oceanography, Numerical Modeling, Mesoscale

Disiplinary signature	Responsible signature
Lars Anders Breivik, Head Section Ocean and Ice	Øystein Hov, Head Research and Development Department

Postal address PO Box 43 Blindern, N-0313 Oslo, Norway
Office Niels Henrik Abels vei 40
Telephone +47 2296 3000
Telefax +47 2296 3050
e-mail: met.inst@met.no **Web:** met.no
Bank account 7695 05 00601
Swift code DNBANOKK

[1]Norwegian Meteorological Institute
[2]Institute of Marine Research

Executive summary

Group: We are the Norwegian Meteorological Institute (contractor) and the Institute of Marine Research (subcontractor), hereafter the met.no/IMR group.

Contract: We have performed the above under a contract by and between StatoilHydro (now Statoil) and the Norwegian Meteorological Institute (Contract No. 4501790631).

Objective: To decide on a new model version for ROMS, and to provide the necessary model results for a third party to assess whether the new version performs better than the previous used in Phase 2 (*Røed et al.*, 2007; *ForOcean*, 2008). Also the effect of using a higher resolution atmospheric forcing is studied. The third party assessment may be found in *ForOcean* (2010).

Why ROMS?: We have opted for using ROMS mainly because an earlier comparison study by *LaCasce et al.* (2007) concluded that ROMS was superior, a result corroborated by *ForOcean* (2008). We believe that one of the main reasons for this is the more advanced numerical methods employed giving an effective increased resolution for a given grid size compared to other models, and that it employs a generalized terrain-following coordinate that allows high vertical resolution near the surface even in the deep water areas (cf. *Haidvogel et al.*, 2008; *Shchepetkin and McWilliams*, 2005, 2009). Furthermore it helps us to mitigate the common pressure gradient error plaguing models employing the traditional terrain-following coordinate.

Work done: We perform ten tidal tests and three three year long full trial hindcasts as base for deciding on a new version of ROMS. The new version contains tidal nodal corrections and a few other upgrades. The model system is as in Phase 2, that is, we nest a 4 km mesh model covering the Barents and Kara Seas (innermost model) into a coarser mesh model covering the North Atlantic (*Røed et al.*, 2007). Only the innermost model is replaced with the upgraded and corrected version. The lateral boundary input is thus the same as in Phase 2. We first assessed the results from the many tests and trial hindcasts. In this we were guided by the model deficiencies revealed by *ForOcean* (2008). We then performed two full one-year-long hindcasts. The first is forced as in Phase 2, while the second is forced using the higher resolution atmospheric input described in *Reistad et al.* (2009) and *Reistad et al.* (2011).

Conclusions: We experienced no major technical problems during the hindcast runs. Based on the results we conclude that the model does give better ice conditions and residual currents, but that the model is still imperfect regarding tidal predictions. We think there are a number of reasons for this. First, there is an error in the AOTIM tidal data base (*Padman and Erofeeva*, 2004) used at the open boundaries as forcing. Second the Barents Sea is particularly sensitive because the M_2 tidal constituent has a frequency close to the inertial frequency. Third, the tides are sensitive to errors in topography because tidal waves propagate with a speed proportional to the square root of the depth. Finally, also residual currents are sensitive to topography errors because shoals and banks may not be properly represented. The latter is particularly relevant since shoals are precisely what we are not resolving with the bathymetry used in KARBIAC, and currents tend to scale nearly inversely to the depth.

Contents

Abbreviations used in the text

- AOTIM = Arctic Ocean Tidal Inverse Model (*Padman and Erofeeva*, 2004)
- CCSM = NCAR's Community Climate System Model
- CCSM4 = Version 4 of CCSM
- COARE = Coupled Ocean-Atmosphere Response Experiment
- GLS = Generic length Scale
- HIRLAM = High Resolution Limited Area Model
- KARBIAC = KARa and Barents Sea Ice And Current
- KARBIAC model = The version of the model ROMS set up for the KARBIAC project
- IMR = Institute of Marine Research, Bergen, Norway
- JIP = Joint Industry Project
- NCAR = National Center for Atmospheric Research, Boulder Colorado, USA.
- NWP = Numerical Weather Prediction
- met.no = The Norwegian Meteorological Institute, Oslo, Norway
- met.no/IMR group = The modeling group consisting of met.no and IMR
- MIPOM = Norwegian Meteorological Institute's version of the Princeton Ocean Model referred to as frequency diagrams
- POM = Princeton Ocean Model
- ROMS = Regional Ocean Modeling System
- www.yr.no = The Norwegian Meteorological Institute web portal for dissemination of atmospheric and ocean weather forecasts
- SIC = Sea Ice Concentration
- SST = Sea surface temperature
- SSH = Sea surface height. Contains the combined water level due to tides and storm surges.
- TPXO = The Oregon State University TOPEX/POSEIDON Global Inverse Solution

1 Purpose and scope

1.1 Background

To prepare for eventual oil and gas exploration in the KARBIAC area it is of general importance to get a good understanding of the environment. In particular, it is of interest to get insight into the meteorological and oceanographic variables such as winds, waves, water level (tidal height and storm surge) and currents to design offshore structures that are both safe and cost efficient. Accordingly, the overall aim of the KARBIAC JIP is to produce sufficiently accurate information about long-term cycles and trends, in particular with regard to currents and sea ice. The latter shows strong interannual and interdecadal variability, and hence records of 20 to 40 years duration are needed (*Kvingedal*, 2005; *Sorteberg and Kvingedal*, 2006). The only means by which such time series can be provided is by performing long-term hindcasts using numerical ocean models.

Before embarking on such an endeavor it is of considerable interest to assess the skill of the ocean model to be employed. The KARBIAC JIP therefore decided to perform a project (KARBIAC Phase 2) in which results from three different model hindcasts performed by three different modeling groups were assessed for a trial period of one year (July 1, 1987 through April, 1988). Prior to Phase2 the participating models and modeling groups were first selected through a qualification Phase (KARBIAC Phase 1).

The results from the various modeling groups were assessed by a third party who compared the model results with measurements at up to 29 sites in the Barents Sea (*ForOcean*, 2008). Based on this comparison report the KARBIAC participants judged the results delivered by the modeling group consisting of the Norwegian Meteorological Institute and the Institute of Marine Research (hereafter the met.no/IMR group) using the ROMS model to be the most accurate. The work performed by them in Phase 2 is reported in *Røed et al.* (2007).

However, some deficiencies regarding the tidal signal in ROMS were discovered and reported by *ForOcean* (2008). Based on this assessment the KARBIAC participants decided to ask the met.no/IMR group to perform an intermediate hindcast project, referred to as KARBIAC Phase 2b. The results of the latter project are reported here.

1.2 Scope of work Phase 2b

The scope of work for Phase 2b work consists of the following activities:

1. To make corrections and upgrades to the Phase 2 model version of ROMS and perform new trial hindcasts to assess the impact of these upgrades and corrections in general and on the tidal signal in particular.

2. To decide on a new model version.

3. To perform two new one-year long hindcasts with the new model version, one with atmospheric forcing as in Phase 2 (ERA40 reanalysis, henceforth ERA40), and a second using a higher resolution (10 km mesh size) atmospheric forcing as described in *Reistad et al.* (2009, 2011) (henceforth HL).

4. To deliver time series and sea-ice fields extracted from the two new hindcasts. The variables to be extracted are water level (tides and storm surges), horizontal current components, temperature and salinity. The sea-ice fields delivered are ice concentration, ice thickness and ice age. Ice velocity is calculated, but not asked for (no data for comaparison).

5. To write this final report.

6. To assess whether the results from the two new hindcasts with the new model version are better than the Phase 2 hindcast results, in particular with regard to tides. This assessment was done by a third party (*ForOcean*, 2010).

Regarding item 1 we perform ten shorter runs and three three-year long hindcasts. This is deemed necessary to be able to assess the full impact of the changes made. Although not contractually obligated, we also decided to extend the two hindcasts mentioned in item 3 to cover the full year of Phase 2, that is, May 1, 1987 through April 30, 1988. The rationale is to provide a better base for a proper comparison with the results of Phase 2. Accordingly the time series in item 4 covers the entire Phase 2 hindcast period. A spin-up period of half a year prior to the hindcast period are added to these runs, but is not considered. Finally, we emphasize that although we employ the same doubly-nested model system as in Phase 2 (cf. Figures 1 and 2), we only employ the new ROMS version for the innermost, fine mesh model in the doubly-nested system. Thus the lateral forcing conditions at the open boundaries of the fine mesh model are the same as those in Phase 2.

1.3 Why ROMS?

Our model of choice for the KARBIAC project is the ocean model ROMS. Essential in this choice is that a comparison study of ROMS and two other ocean models for an area off West Norway, concluded that ROMS was superior (*LaCasce et al.*, 2007)[3]. We were therefore pleased that the KARBIAC participants, based on the comparison analysis of *ForOcean* (2008), reached the same conclusion. Moreover, we chose ROMS because it employs a modified terrain-following coordinate allowing high vertical resolution near the surface even in the deep water areas (*Haidvogel et al.*, 2008; *Shchepetkin and McWilliams*, 2005, 2009). In addition the modified vertical coordinate helps to mitigate the pressure gradient error plaguing models employing the traditional terrain-following coordinate (the so called σ-coordinate).

1.4 Organization of report

In Section 2 we describe the corrections, changes and updates we have made to the Phase 2 version of ROMS, some of the tests made and the results thereof. We also include in Section 2 a brief description of the new atmospheric input provided by the archived HIRLAM 10 km

[3]This comparison study, funded through the so called CONMAN project, was initiated by the offshore companies within the JIP named the Norwegian Deepwater Project that included the four participants in the present JIP.

analyses. In Section 3 we describe the model results delivered for assessment and give some sample results. Finally, we provide a summary (Section 4) and an Executive summary (cf. page i).

2 The new model version

In setting up the KARBIAC version of ROMS for the two one-year hindcasts there is some crucial external input needed. This includes definition of the computational domain and the topography. Other important input is mesh size, atmospheric driving forces (momentum, freshwater and heat fluxes), input from rivers, tidal forcing, initial conditions and lateral forcing at open ocean boundaries.

For Phase 2b we have kept the external input as described in *Røed et al.* (2007), except for Case HL where we have replaced the atmospheric driving forces of Phase 2 and Case ERA40 with the atmospheric driving forcing from the recently established hindcast archive for wind and waves described in *Reistad et al.* (2009) and *Reistad et al.* (2011). The latter provides atmospheric input on a 10 km grid based on the NWP model HIRLAM which constitutes a much higher resolution for the atmospheric forcing.

There are also a number of important internal model considerations to be made, e.g., choice of parameters and options for the modified vertical coordinate, choice of advection scheme, choice of bottom friction, etc. These are described as we go along.

In this Section we describe the various tests we have performed, the test results and conclusions therefrom as this is the basis for the final choice of model version to use for the two hindcast runs referred to as Case ERA40 and Case HL, respectively. Thus all the test cases and runs described in this section use the ERA40 reanalysis as atmospheric input for the atmospheric driving forces.

The tests we have performed may be separated in two parts as follows.

1. Three full runs for three years covering the period 1.1.1986 through 31.12.1988. They are henceforth referred to as Reference, CCSM and TB4, respectively.

2. Ten shorter runs of length one to two months focusing on testing the impact on the tidal signal to various model parameters and parameterizations.

2.1 The three full runs

As alluded to all the three full runs are for three years of which the first one and a half years are considered being a spin-up period. The lateral boundary forcing and initial conditions are taken from the 20 km North Atlantic model run as part of the doubly-nested system of Phase 2 (cf. Figure 1). Thus only the nested high resolution domain is rerun.

2.1.1 Reference solution

For the first full run, the Reference, we first of all downloaded the most recent version of the coupled ice-ocean model ROMS. Regarding the terrain-following vertical coordinate σ we

opted to use the new and more robust vertical coordinate transform and stretching suggested by *Shchepetkin and McWilliams* (2005, 2009) rather than the one we used in Phase 2 suggested and described by *Song and Haidvogel* (1994). This new transform makes it possible to maintain almost equidistant distribution of vertical levels (in geopotential coordinates) in the upper mixed layer even in deeper waters. At the same time it provides the possibility of maintaining a high resolution in the bottom boundary layers.

The stretching parameters we use in Reference are $\theta_s = 8$ and $\theta_b = 0.9$[4]. This gave us nearly horizontal σ surfaces and high resolution in the upper mixed layer (upper 50 m) and a strong bottom-following constraint.

We also corrected for errors made in the prescribed time reference for tidal epoch and Greenwich phase of tides. Regarding vertical levels we kept the number to 35 as in Phase 2. We also used the Generic length Scale (GLS) $k-\omega$ turbulence model of *Umlauf and Burchard* (2003).

Finally, we opted to replace the uniform linear friction factor with one varying spatially. We determined the factor from the root mean square current speeds in a preliminary one-year long simulation using the same atmospheric forcing as in Phase 2.

2.1.2 CCSM solution

For the second full run, the CCSM, we replaced the bulk flux algorithm used for atmospheric forcing in the Reference [5] to the new bulk flux algorithm for atmospheric forcing used in the NCAR Community Climate System Model (CCSM) for high latitudes. These were applied to the momentum fluxes and the latent and sensible heat fluxes. The long- and short-wave radiative fluxes and precipitation-evaporation (freshwater fluxes) are unchanged. Nothing else was changed.

2.1.3 TB4 solution

In the third and final full run we test the impact of loosening the coupling to the ocean bottom. Accordingly we changed the vertical transform bottom parameter θ_b in the CCSM solution from $\theta_b = 0.9$ to $\theta_b = 0.4$. The rationale is to test if bottom currents are improved in areas entertaining a steep shelf slope. This is also a test to see if vertical current profiles have degraded accuracy with poorer resolution in the bottom boundary layer.

2.1.4 Results from the full runs

The results in terms of sea ice concentration (SIC) and sea surface temperature (SST) on April 11, 1988 are given in Figures 3, 4 and 5. For comparison are also plotted the similar results from Phase 2 in terms of SIC (Figure 3) and SST (Figure 5). In Figure 4 is the SIC compared to the observed SIC as extracted from *ForOcean* (2008).

In summary, the SICs in general look improved over the Phase 2 results. Changing bulk flux algorithm (CCSM vs. COARE) alters the SIC as well as the SST. We observe that CCSM

[4] See *Shchepetkin and McWilliams* (2009) for details

[5] The ROMS default is the COARE bulk flux formulation as described in *Fairall et al.* (2003).

and TB4 are quite similar and that all three full runs differ from the Phase 2 result. In particular we note that the warmer water in CCSM and TB4 now extends further north along the western shores of the Svalbard Archipelago and further east into the Barents Sea improving the SIC extent to be more in line with the observed one. Changing vertical resolution near the bottom appears to have no detectable effect on the SIC and the SST (TB4) in comparison with the CCSM. Thus we conclude that replacing the COARE bulk flux algorithms with the CCSM algorithms has a positive effect on the SIC and SST indicating that the CCSM bulk flux algorithms should replace the default algorithms used in ROMS.

2.2 Tidal simulations

In addition to the three full runs described in Section 2.1 we also ran ten shorter (1-2 month) simulations focusing on the tidal response. Thus, in all, results from 13 simulations have been examined regarding the tidal response. In Phase 2 the ROMS M2 tidal currents were typically 20% too large, K1 tidal currents generally too small. We have carried out several short (1-2 month) simulations to investigate what might be causing the over-estimation of M2 tidal currents.

Table 1 lists the thirteen runs made to examine the effect of type and magnitude of bottom friction, turbulence closure scheme, bottom resolution, type and magnitude of boundary tidal forcing on the tidal response. Note that the first three are the full runs.

2.2.1 Results from the tidal examination

To assess the impact of the changes we need observations. Since we don't have access to the tidal analyses of the observations, we took the station 12 results from *ForOcean* (2008) (corresponds to ZT-13 (*ForOcean*, 2008)). The comparison is given in Table 2.

From Table 2 we conclude that the greatest sensitivity is to errors in tidal forcing at the open boundaries. We also conclude that we need to do an assessment of Arctic Ocean Tidal Inverse Model (AOTIM) data in the study area. We also find that bottom drag formulation and, to lesser extent, the turbulence model have significant impact on magnitude of near-bottom currents. However, very little impact is detected in "free-stream" water parcels.

The primary cause appears therefore to be inaccuracies in the tidal boundary forcing. The secondary cause is inaccuracies in bathymetry. However, in another project regarding construction of a Lowest Astronomical Tide for the Nordic Seas using our ROMS version they noted that the Barents Sea tides were the most difficult to get correct (Ann Kristin Sperrevik, personal communication). This is despite the fact that she used a different tidal data base, namely the TOPEX/POSEIDON Global Inversion Solution (TPXO) tidal data base of Oregon State University (*Egbert et al.*, 1994; *Egbert and Erofeeva*, 2002)[6]. This indicates that topography may be more important than exhibited here. It should also be mentioned that at the latitudes covered by the Barents Sea the M_2 tidal frequency and the inertial frequency are equal, and this may have an effect as well.

[6]TPXO is the current version of a global model of ocean tides, which best-fits, in a least-squares sense, the Laplace Tidal Equations and along track averaged data from TOPEX/Poseidon and Jason (on TOPEX/POSEIDON tracks since 2002) obtained with OTIS http://volkov.oce.orst.edu/tides/global.html

2.3 The Phase 2b model

Based on these results we decided on the following set-up for the new model version of ROMS to be used in the two new hindcasts ERA40 and HL of Phase 2b.

We replace the vertical transform of *Song and Haidvogel* (1994) with that suggested and described by *Shchepetkin and McWilliams* (2005, 2009) (for insiders this means setting the parameters $Vtransform = Vstretching = 2$). The other parameters in the vertical transform were set as follows: *hmin* = 10m, $Tcline$ = 50m, $\theta_s = 8$, $\theta_b = 0.4$. We also use the CCSM atmospheric bulk flux algorithms. Finally, based on the tidal simulations as given in Table 2 we reduced the M_2 amplitude on the open boundaries by 7%, that is, somewhat in between what simulations nos. 0.92UVZ and 0.943M2Z suggest (cf. Table 1).

3 The ERA40 and HL hindcasts

As mentioned two new one-year long hindcasts were produced, referred to as ERA40 and HL, respectively. Both use the same new model version as described in the previous Section. They differ only in the atmospheric forcing. While ERA40 uses the same forcing as in Phase 2, the HL hindcast uses atmospheric input extracted from the recently established 10 km hindcast archive of wind and waves as described in *Reistad et al.* (2009) and *Reistad et al.* (2011). This archive is based on the HIRLAM NWP model.

One problem was encountered regarding the HL hindcast. The domain covered by the HL hindcast did not match completely with the KARBIAC model domain, with the latter extending a bit further north. However, the part outside of the HL domain was small and thus we felt safe ameliorating the situation by merging the ERA40 and the hindcast archive in this small area.

3.1 Time series and ice concentration fields delivered

The agreed upon model results from the ERA40 hindcast were delivered to Statoil in December 2009 and the model results from the HL hindcasts in January, 2010. An explanation of the files containing the delivered model results is provided in the Appendix. The model results were analysed by a third party and are found in *ForOcean* (2010).

3.2 Results

We now briefly present some of the results from the two hindcasts focusing on the same stations as presented in the Final Report to KARBIAC Phase 2 (*Røed et al.*, 2007), that is, stations 10 and 26. Station 10 is close to Bear Island while station 26 is the north-eastern most station close to Novaja Zemlya (Figure 6).

3.2.1 Ice extent and concentration

We first examine the ice concentrations from the three hindcasts at March 28, 1988 as displayed in Figure 7. At first glance these ice extent and concentration fields appear quite

similar. A more detailed examination reveals some differences at the entrance to the Kara Sea and some differences in the north-eastern part of the domain shown. The Phase 2 and ERA40 hindcasts seem to have about the same somewhat high concentration at the entrance to the Kara Sea, while the HL hindcast shows a lower ice concentration. The extent is about the same in all three. In the north-eastern part it is the HL and Phase 2 hindcasts that are similar while the ERA40 differs (lower ice concentration). The ice pattern in ERA40 and HL is however more similar, and both differ from Phase 2.

3.2.2 Current statistics at station 10 and 26

The current statistics for station 10 and 26 from the Phase 2 hindcast are presented in Figures 8 and 12, respectively (reproduced from *Røed et al.*, 2007). The frequency diagrams (probability distributions or PDFs) may be compared with the PDFs, scatter and rotational scatter plots from the two new hindcasts ERA40 and HL as displayed in Figures 9 and 15.

Examining the PDFs at station 10 (Figure 9) we find that the surface and mid depth distributions of hindcasted speeds and directions are very similar for the two hindcasts, and also similar to the Phase 2 hindcast. All hindcasts show a reduction in mean speed and a shift in peak direction toward the bottom , but HL has slightly less energy at the high speeds. We observe that the high resolution atmospheric forcing tends to give more of a spread in the directional PDF at the bottom.

Examining the similar products for station 26, as depicted in Figures 12 - 15, we again find that the PDFs are quite similar, and that the current speeds are reduced toward bottom. We also note that the currents are rectilinear in that all the directional PDFs has two peaks at the same angle. We also observe that there is a puzzling inconsistency in current direction when comparing the two new hindcasts with Phase 2 (Figure 8). While the direction in the two new hindcasts are aligned with the topography at station 26, the direction sepicted in Figure 8 entails cross isobath currents.

4 Summary and conclusions

We report on the work done by the Norwegian Meteorological Institute, Oslo, Norway and the Institute of Marine Research, Bergen, Norway (the met.no/IMR group) associated with Phase 2b of the KARBIAC JIP.

The goal of the present work is first to decide on a new and improved version of the ROMS model and second to produce two new one-year hindcasts using the new version of ROMS. The new hindcasts differ only in the atmospheric forcing applied. The first applies the relatively low resolution ERA40 reanalysis, while the second applies the atmospheric forcing extracted from the recently established, high resolution HIRLAM 10 km wind and wave hindcast archive (*Reistad et al.*, 2009, 2011). As before, the results were delivered to a third party for an independent assessment. The goal of the assessment is twofold. The first is to investigate whether the new ROMS version performs better than the version used in Phase 2 as reported earlier in *ForOcean* (2008). The second is to assess the impact of using a higher resolution

atmospheric forcing. The conclusions of the third party assessment is reported in (*ForOcean*, 2010).

The ocean model ROMS was originally chosen because an earlier study by *LaCasce et al.* (2007) concluded that ROMS was superior to two other models. Furthermore, it is chosen because it employs a modified terrain-following coordinate. This modification allows high vertical resolution near the surface even in the deep water areas, and helps to mitigate the pressure gradient error plaguing models employing the traditional terrain-following coordinate (the so called σ-coordinate) (*Haidvogel et al.*, 2008; *Shchepetkin and McWilliams*, 2005, 2009). As mentioned by *LaCasce et al.* (2007) we underscore that the main reason for the success of ROMS was that it employs more sophisticated numerics than many other ocean models.

To decide on a new version we first downloaded the most recent version of the coupled ice-ocean ROMS model available to us. We then opted for using the new vertical transform suggested by *Haidvogel et al.* (2008); *Shchepetkin and McWilliams* (2005, 2009) and produced a full three-year run with this model version[7]. Two more full three-year runs were done. In the first we replaced the default bulk flux algorithms of ROMS with those in NCAR's CCSM4 model. In the second we loosened the strong bottom coupling used in the two first full three-year runs. Thereafter we ran ten shorter hindcasts (one to two months long) testing various options (cf. Table 1). Using the observed tides at one station as guideline we finally decided on a new version. The new version employs the new vertical transform and the NCAR CCSM4 bulk flux algorithms. Finally it apples a 7% reduction for the M_2 tidal component forcing on the lateral boundaries.

We then performed two new hindcasts with this model version using the two different atmospheric forcings as described in the second paragraph of this Section. As for Phase 2 the main model output is in terms of total water level (tides and storm surges), two horizontal current components, temperature, salinity, ice concentration, ice thickness, ice speed and direction and ice age. For conclusions regarding the assessment of the model skill the reader is referred to *ForOcean* (2010). We experienced no major technical problems during the hindcast runs, supporting the conclusion that the new model is indeed technically robust.

Finally, we conclude that the new model version gives better ice conditions and residual current statistics (PDFs), but that it is still imperfect regarding tidal predictions. The primary cause appears to be inaccuracies in the AOTIM tidal boundary forcing (*Padman and Erofeeva*, 2004). It should be emphasized that we inadvertently made an error regarding the phase for tidal input in the ERA40 hindcast resulting in a 180^o phase error for this hindcast, an error that was corrected when performing the HL hindcast (cf.. Table 6.1 of *ForOcean*, 2010). This error may be ameliorated by replacing the AOTIM tidal data base with the TPXO tidal data base (*Egbert et al.*, 1994; *Egbert and Erofeeva*, 2002). The latter tidal data base is in fact, partly due to our KARBIAC experience, presently the standard tidal data base for the ROMS version we use within the met.no/IMR group, and is for instance used by *Røed and Kristensen* (2010, 2011) in their recent studies regarding eddy generation and circulation in the Lofoten-Vesterålen area. We are, however, aware (Ann Kristin Sperrevik, personal communication)

[7]The hindcasts were actually longer due to the necessity of spinning up the model before extracting model results.

that when she used the met.no/IMR group's version of ROMS to construct the Lowest Astronomical Tide for the Nordic Seas using the TOPX tidal data base, she experienced that the tides in the Barents Sea tides were the most difficult to get correct, and in fact never got them quite correct.

Thus topography may be a secondary cause for tidal errors, and more important than exhibited here. We note that the tides are sensitive to errors in topography because tidal waves propagate with a speed proportional to the square root of the depth. Finally, we emphasize that also residual currents are sensitive topography errors because shoals and banks may not be properly represented. The latter is particularly relevant since shoals are precisely what we are not resolving with the bathymetry used in KARBIAC, and currents tend to scale nearly inversely to the depth. Thus we do not expect any skill when comparing observations and model resuslts at locations where the depth is less than say 15 meters.

Acknowledgment

This work was supported in parts by StatoilHydro Petroleum AS (now Statoil), under Contract No. 4501790631. Statoil acts on behalf of a consortium of offshore industry companies (Statoil, Total, Chevron and Shell). The work is part of the Joint Industry Project (JIP) known as KARBIAC. The computations were performed at the Norwegian Supercomputer facilities. We are grateful for the help offered by Nils Melsom Kristensen in preparing some of the graphs.

Appendix

Results extracted from the ROMS model run

Written by Jon Albretsen, W. Paul Budgell and Lars Petter Røed

The model results are delivered as ascii files. They contain time series from the 29 station as agreed upon, and the ice concentration fields.

Time series

The time series range from May 1, 1987 to May 1, 1988 and resolution is one hour. The generic files

ROMS_station_<STATION NO.>_sigmalevel_<SIGMA LEVEL>.dat

contain time series of the depth dependent variables.

STATION NO. indicates which station from the position-list (from 01 to 29).

SIGMA LEVEL indicates which sigma level from the model output. It varies from 35 (surface) to 01 (bottom). Due to the model's enhanced resolution in the vertical near the surface and the bottom, the upper (35) and lower (01) sigma level can be regarded as surface and bottom values, respectively. The columns in the file is explained in Table 3.

Depth profiles

The files with the generic name

ROMS_station_<STATION NO.>_depthprofile.dat

contain the depth profile for each station, that is, the actual depth (z-level) for each σ level (SIGMA LEVEL). The calculation of the depth profile is based on the equilibrium depth and the one year mean of surface elevation at the location of the station.

Surface variables

The generic files named

ROMS_station_<STATION NO.>_surface.dat

contain time series of the depth independent (surface) variables. The files contain the columns explained in Table 4.

Ice concentration fields

The files of generic names

roms_aice_<DATE>.asc

contain ice concentration from all grid points within the area 68-78N and 16-56E. DATE is either 19870907, 19870914, 19870921, 19870928, 19880328, 19880405, 19880411, 19880418 or 19880425. The files contain the columns explained in Table 5.

References

Egbert, G. D., and S. Y. Erofeeva (2002), Efficient inverse modeling of barotropic ocean tides, *J. Atmos. Oceanic Tech.*, *19*(2), 183–204, doi:10.1175/1520-0426(2002)019¡0183:EIMOBO¿2.0.CO;2.

Egbert, G. D., A. F. Bennett, and M. G. G. Foreman (1994), Topex/poseidon tides estimated using a global inverse model, *J. Geophys. Res.*, *99(C12)*, 24,821–24,852, doi: 10.1029/94JC01894.

Fairall, C. W., E. F. Bradley, J. E. Hare, A. A. Grachev, and J. B. Edson (2003), Bulk parameterization of air-sea fluxes: Updates and verification for the COARE algorithm, *J. Clim.*, *16*, 571–591, doi:10.1175/1520-0442(2003)016<0571:BPOASF>2.0.CO;2.

ForOcean (2008), Kara and Barents Seas Ice and Current (KARBIAC) Joint Industry Project: Comparison of Hindcasts with Measurements, Consultant report to Statoil, February 2008, Foristall Ocean Engineering, Inc.

ForOcean (2010), Kara and Barents Seas Ice and Current (KARBIAC) Joint Industry Project: Phase 2b Comparisons of Hindcasts and Measurements, Consultant report to Statoil, February 2010, Foristall Ocean Engineering, Inc.

Haidvogel, D. B., H. Arango, P. W. Budgell, B. D. Cornuelle, E. Curchitser, E. D. Lorenzo, K. Fennel, W. R. Geyer, A. J. Hermann, L. Lanerolle, J. Levin, J. C. McWilliams, A. J. Miller, A. M. Moore, T. M. Powell, A. F. Shchepetkin, C. R. Sherwood, R. P. Signell, J. C. Warner, and J. Wilkin (2008), Ocean forecasting in terrain-following coordinates: Formulation and skill assessment of the regional ocean modeling system, *J. Comput. Phys.*, *227*(7), 3595–3624, doi:http://dx.doi.org/10.1016/j.jcp.2007.06.016.

Kvingedal, B. (2005), Sea-ice extent and variability in the Nordic Seas, 1967-2002, in *The Nordic Seas: An Integrated Perspective, Geophysical Monograph Series Vol. 158*, edited by H. Drange, T. Dokken, T. Furevik, R. Gerdes, and W. Berger, American Geophysical Union, Washington, DC.

LaCasce, J. H., L. P. Røed, L. Bertino, and B. Ådlandsvik (2007), CONMAN Technical Report No. 2: Analysis of model results, *met.no Report 5/2007*, Norwegian Meteorological Institute, P.O. Box 43 Blindern, 0313 Oslo, Norway, ISSN 1503-8025.

Padman, L., and S. Erofeeva (2004), A barotropic inverse tidal model for the Arctic Ocean, *Geophys. Res. Lett.*, *31*, L02303, doi:10.1029/2003GL019003.

Reistad, M., Ø. Breivik, H. Haakenstad, O. J. Aarnes, and B. R. Furevik (2009), A high-resolution hindcast of wind and waves for the North Sea, the Norwegian Sea and the Barents Sea, *met.no Report 14/2009*, Norwegian Meteorological Institute, Postboks 43 Blindern, N-0313 Oslo, Norway.

Reistad, M., Ø. Breivik, H. Haakenstad, O. J. Aarnes, B. R. Furevik, and J.-R. Bidlot (2011), A high-resolution hindcast of wind and waves for the North Sea, the Norwegian Sea and the Barents Sea, submitted to J. Geophys. Res.

Røed, L. P., and N. M. Kristensen (2010), LOVECUR Final Report: Description of model and discussion of the model results, *Tech. Rep. 21/2010*, met.no Report no., [Available from Norwegian Institute of Air Research, P.O. Box 100, N-2007 Kjeller, Norway].

Røed, L. P., and N. M. Kristensen (2011), Eddy generation and cross shelf mixing in the Lofoten Basin, *In preparation*.

Røed, L. P., W. P. Budgell, J. Albretsen, A. Carrasco, and B. Ådlandsvik (2007), KARBIAC Phase II: Contract no. 4501267762 Final Report, [Available from the Norwegian Meteorological Institute, P.O. Box 43 Blindern, 0313 Oslo, Norway].

Shchepetkin, A. F., and J. C. McWilliams (2005), The Regional Ocean Modeling System (ROMS): A split-explicit, free-surface, topography-following coordinate ocean model, *Ocean Modelling*, *9*, 347–404.

Shchepetkin, A. F., and J. C. McWilliams (2009), Correction and commentary for "ocean forecasting in terrain-following coordinates: Formulation and skill assessment of the regional ocean modeling system" by haidvogel et al., j. comp. phys. 227, pp. 3595-3624, *Journal of Computational Physics*, *228*(24), 8985 – 9000, doi:10.1016/j.jcp.2009.09.002.

Song, T., and D. Haidvogel (1994), A semi-implicit ocean circulation model using a generalized topography-following coordinate system, *J. Comput. Phys.*, *115*, 228–244.

Sorteberg, A., and B. Kvingedal (2006), Atmospheric forcing on the Barents Sea winter ice extent, *J. Clim.*, *19*, 4772–4784.

Umlauf, L., and H. Burchard (2003), A generic length-scale equation for geophysical turbulence models, *J. Marine Res.*, *61*, 235–265.

List of Tables

Table 1: Overview of tidal simulations. Abbreviation in the last column refers to those used in Table 2.

Run #	Name or explanation	Short-name
1	Reference	RS
2	CCSM	CCSM
3	TB4	TB4
4	GLS Mellor and Yamada 2.5 turbulence	k-kl
5	k-kl with surface tide only boundary	Zbc
6	Doubled spatially-varying linear drag	2RDRG
7	Quadratic bottom drag	Qdrag
8	Logarithmic drag z_0=0.002m	Logdrag2
9	Logarithmic drag z_0=0.004m	Logdrag4
10	Reduce tidal boundary forcing 15%	0.85UVZ
12	Reduce tidal boundary forcing 8%	0.92UVZ
13	Reduce surface M_2 tidal boundary forcing 5.7%	0.943M2Z

Table 2: Comparison of simulated tidal response and observations at 10m, 50 m 100m depth and 3m above bottom. The data are from station 12 (ZT13 of *ForOcean*, 2008) and shows the major axis of the M_2 current ellipse in cm/s. Abbreviation used in first column refers to Table 1.

Data set	10m	50m	100m	3m above bottom
Observed	12	15	15.1	8.1
RS	18.1	18.9	19.2	8.2
CCSM	17.5	19.0	19.3	8.1
TB4	18.3	18.6	19.0	8.6
k-kl	18.3	18.5	19.0	9.6
Zbc	18.3	18.5	18.7	11.4
2RDRG	18.4	18.9	19.5	7.7
Qdrag	18.4	18.7	19.3	9.1
Logdrag2	18.2	18.3	18.8	10.0
Logdrag4	18.0	18.2	18.6	9.4
0.85UVZ	11.1	11.4	11.8	5.1
0.92UVZ	14.0	14.5	15.0	6.7
0.943M2Z	17.7	17.9	18.5	8.8

Table 3: Explanation of the columns in the files ROMS_station_<STATION NO.>_sigma-level_<SIGMA LEVEL>.dat.

Column #	Content	Unit
1	Year	-
2	Month	-
3	Day	-
4	Hour	UTC
5	Current speed	m/s
6	Current direction[1]	degrees
7	Temperature	^{o}C
8	Salinity	psu

Note 1: Current direction from the south toward the geographical north has an angle 0, current from the west (east) toward the geographical east (west) has an angle +90 (-90).

Table 4: Explanation of the columns in the files ROMS_station_<STATION NO.>_surface.dat.

Column #	Content	Unit
1	Year	-
2	Month	-
3	Day	-
4	Hour	UTC
5	Tide height[1]	m
6	Storm surge height[1]	m
7	Ice age[2]	days
8	Ice thickness[2]	m
9	Ice concentration[2]	%
10	Ice drift speed[2]	m/s
11	Ice drift direction[2,3]	degrees

Note 1: Tidal and storm surge heights are separated by first performing a harmonic analysis (including 68 constituents) on the one-year time series of total sea level from the model to find the tidal height. The storm surge height is then the tidal height subtracted from the total sea level. Tides in the model consist of amplitude and phase of sea level and depth-mean currents from the eight most dominate constituents (M_2, S_2, N_2, K_2, K_1, O_1, P_1 and Q_1).
Note 2: All ice values were set to zero when ice concentration was below 0.5%.
Note 3: Ice drift direction from the south toward the geographical north has an angle 0, ice drift from the west (east) toward the geographical east (west) has an angle +90 (-90).

Table 5: Explanation of the columns contained in the files roms_aice_<DATE>.asc.

Column #	Content	Unit
1	Longitude	decimal degrees
2	Latitude	decimal degrees
3	Ice concentration[1]	%

Note 1: Minimum value is 0.5%

List of Figures

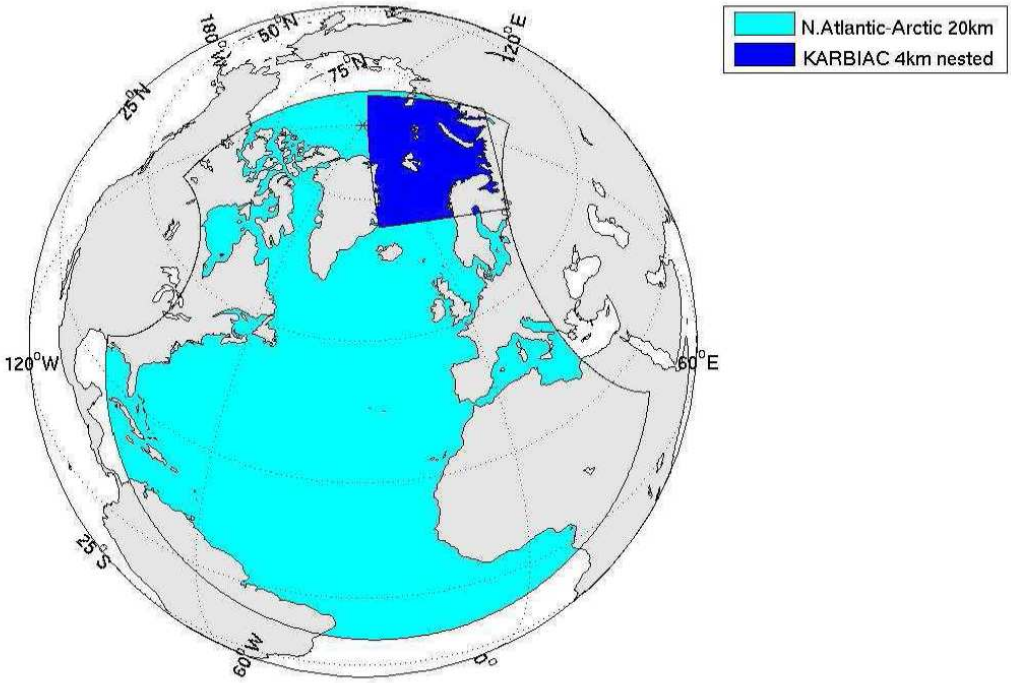

Figure 1: Displayed is the doubly-nested domain used in KARBIAC Phase 2. The fine mesh domain shown in dark blue conforms to the area used in Phase2b, and for which new hindcasts are made (cf. Figure 2). No new hindcasts are produced for the coarse mesh, cyan-colored area (mean grid size 20 km). However, model results from Phase 2 for this latter area are used as lateral boundary conditions for the two new hindcasts of Phase 2b. See Section 1.2 for further explanation.

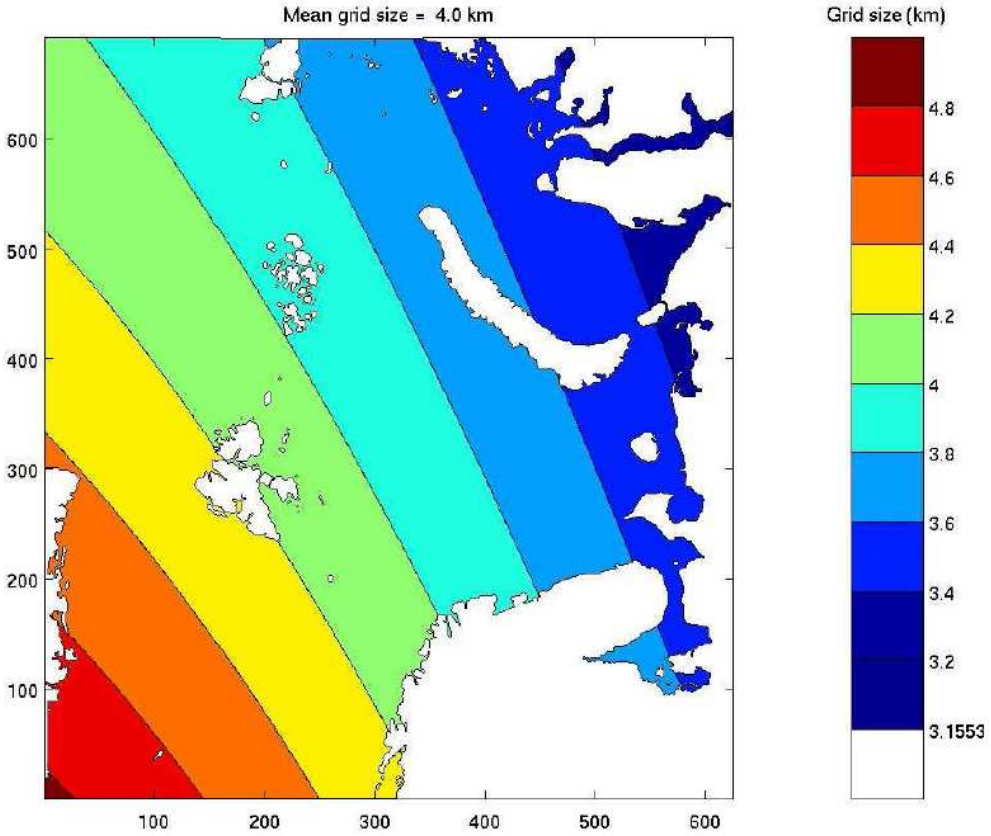

Figure 2: Displayed is the fine mesh model domain of the KARBIAC model. Colors show mesh size as displayed in color bar. The mean grid size is 4 km.

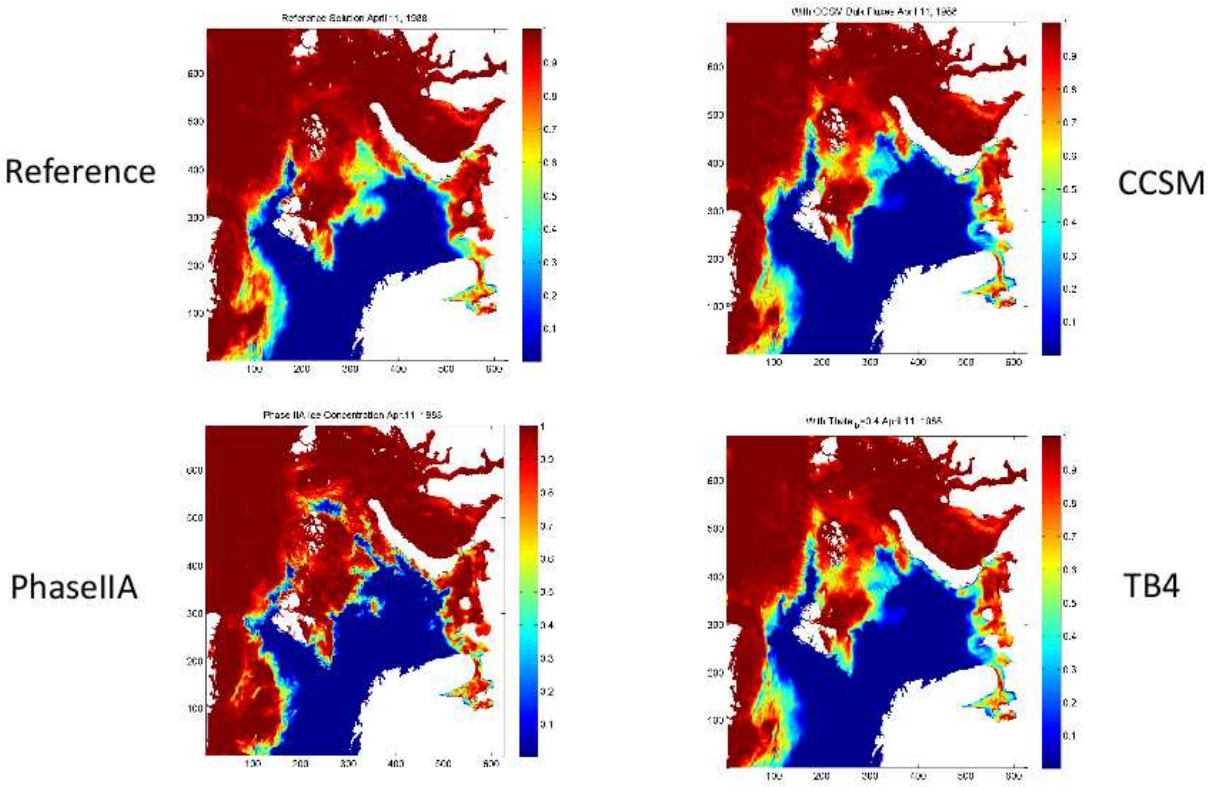

Figure 3: Displayed is the result from the three full runs (marked Reference, CCSM and TB4 in accord with Table 1, respectively) on April 11, 1988 in terms of the sea ice concentration. Also shown for comparison is the similar result from the earlier Phase 2 hindcast (marked Phase IIA).

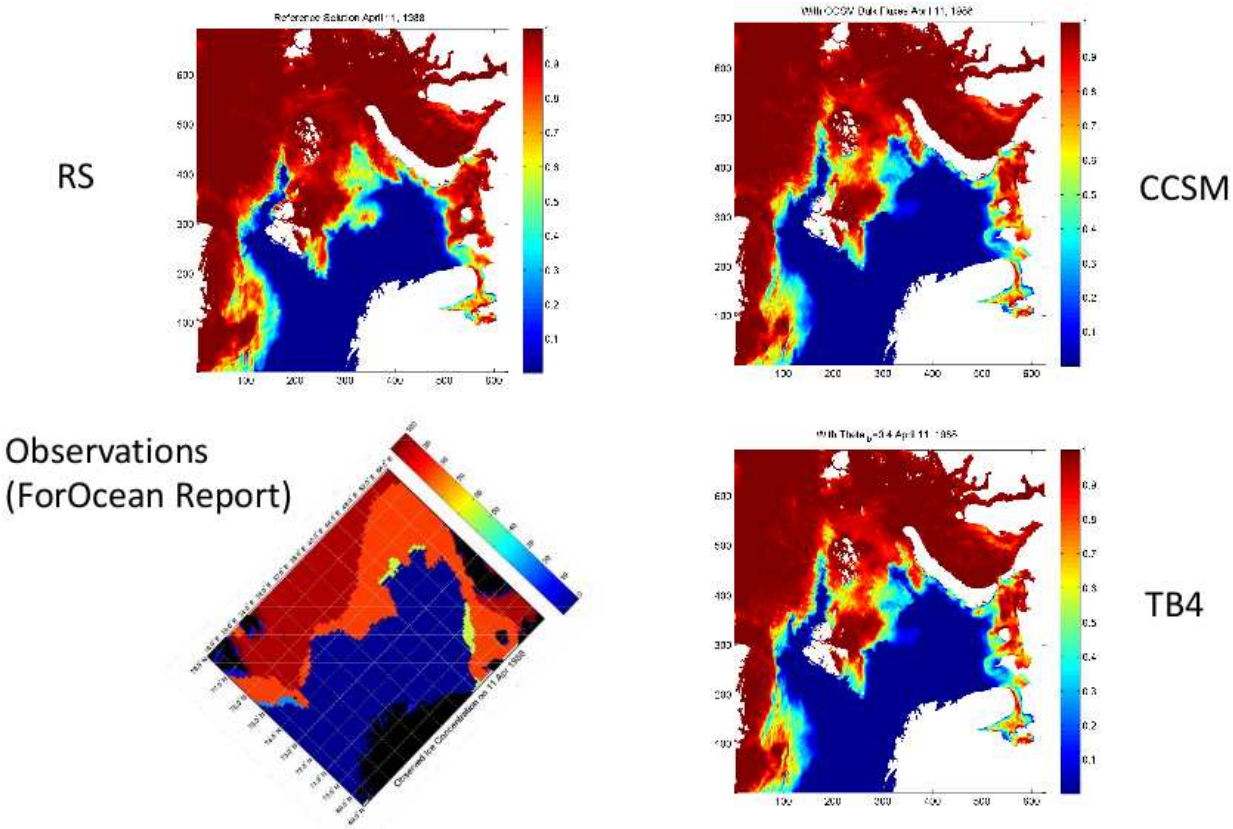

Figure 4: Displayed is the result in terms of sea ice concentration from the three full runs (marked RS, CCSM and TB4 in accord with Table 1, respectively) on April 11, 1988. Also shown for comparison is the similar observational product extracted from *ForOcean* (2008) (marked Observation (ForOcean Report)).

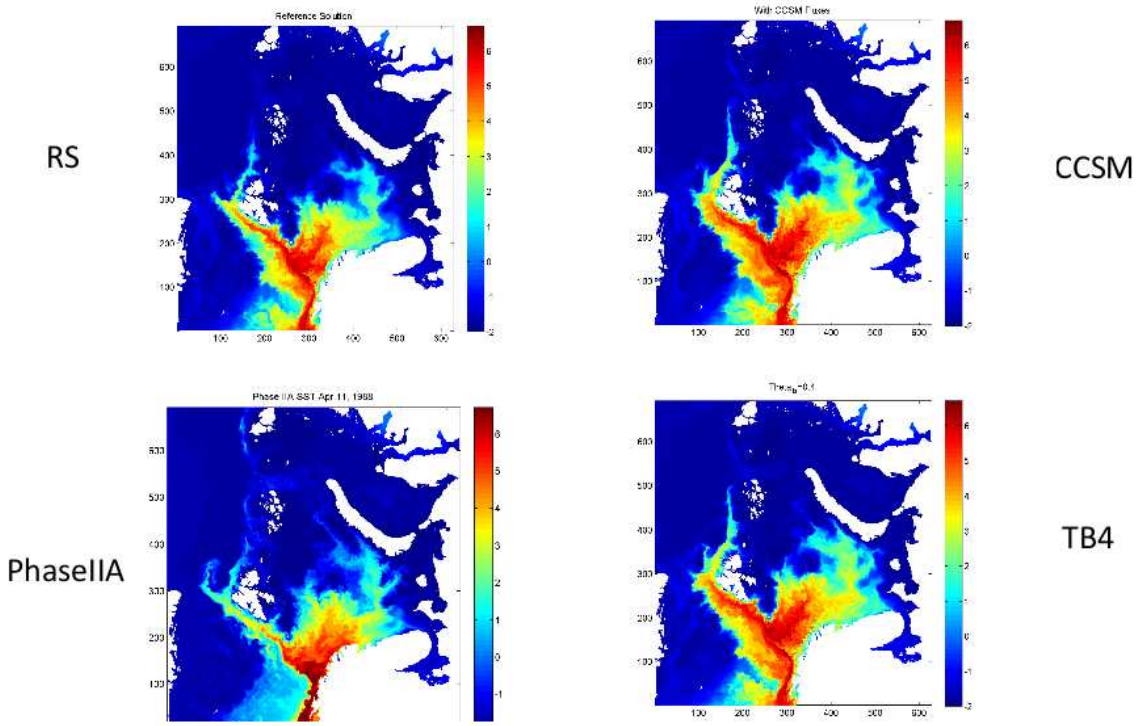

Figure 5: Displayed is the result from the three full runs (marked RS, CCSM and TB4 in accord with Table 1, respectively) on April 11, 1988 in terms of the sea surface temperature (SST). Also shown for comparison is the similar result from the earlier Phase 2 hindcast (marked Phase IIA).

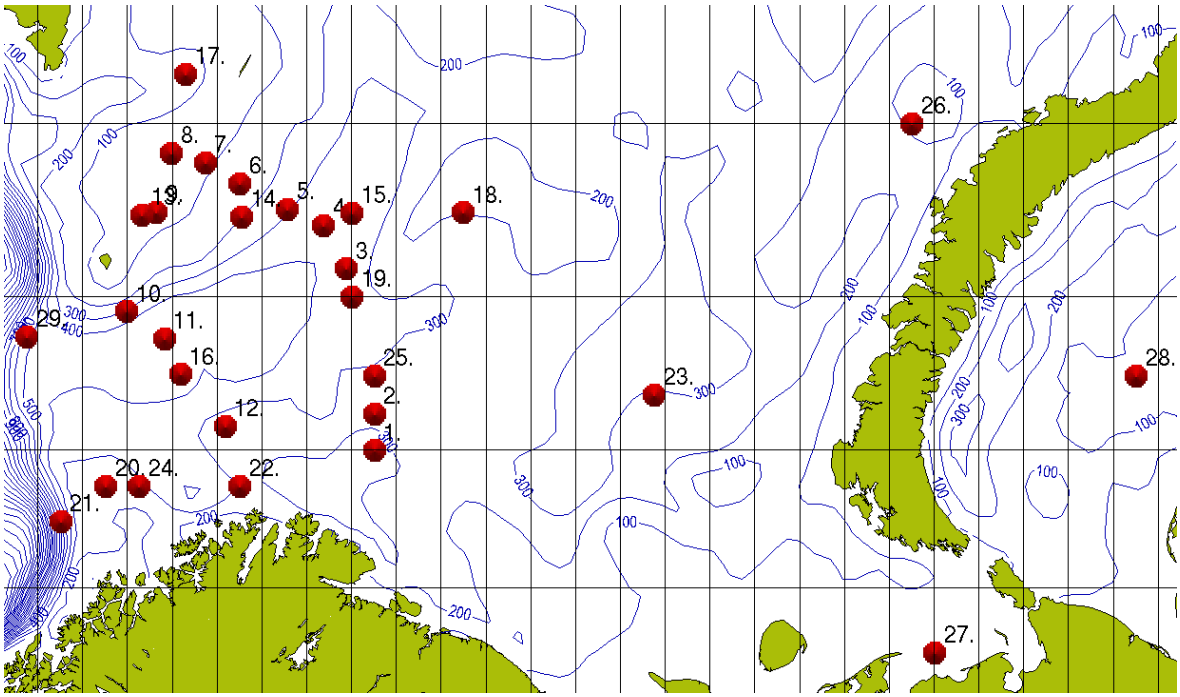

Figure 6: Displayed is a map of the Barents and Kara Seas showing the location of the 29 stations (red circles) where time series of model results were extracted. Also shown are isobaths (blue curves) with contour interval 100m. Solid black straight lines depict the latitude and longitude with a 2^o resolution.

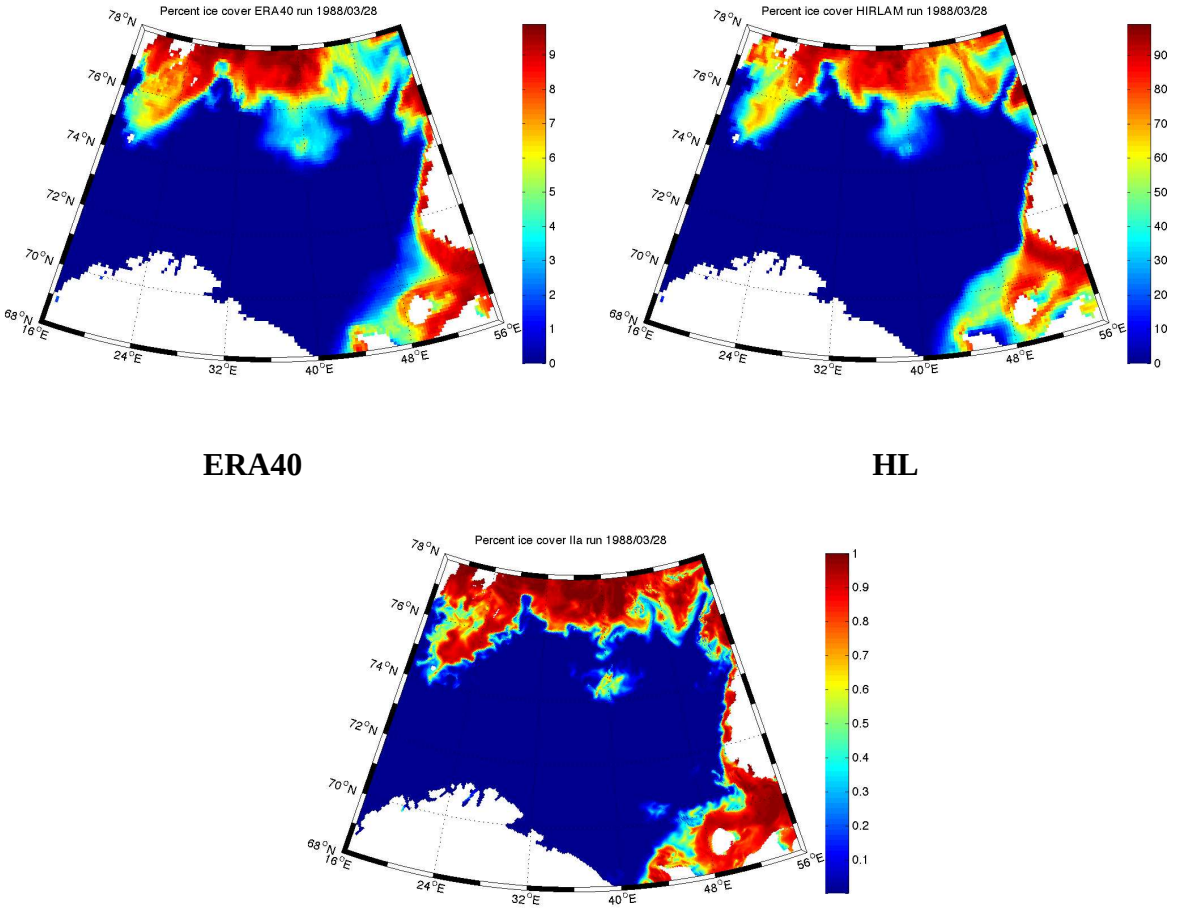

ERA40 **HL**

Phase 2

Figure 7: Displayed is the ice concentration on March 28, 1988 from the two new hindcasts ERA40 and HL (upper panel left and right, respectively) and the Phase 2 hindcast. Colors show ice concentration in one tenth fractions as indicated by color bar.

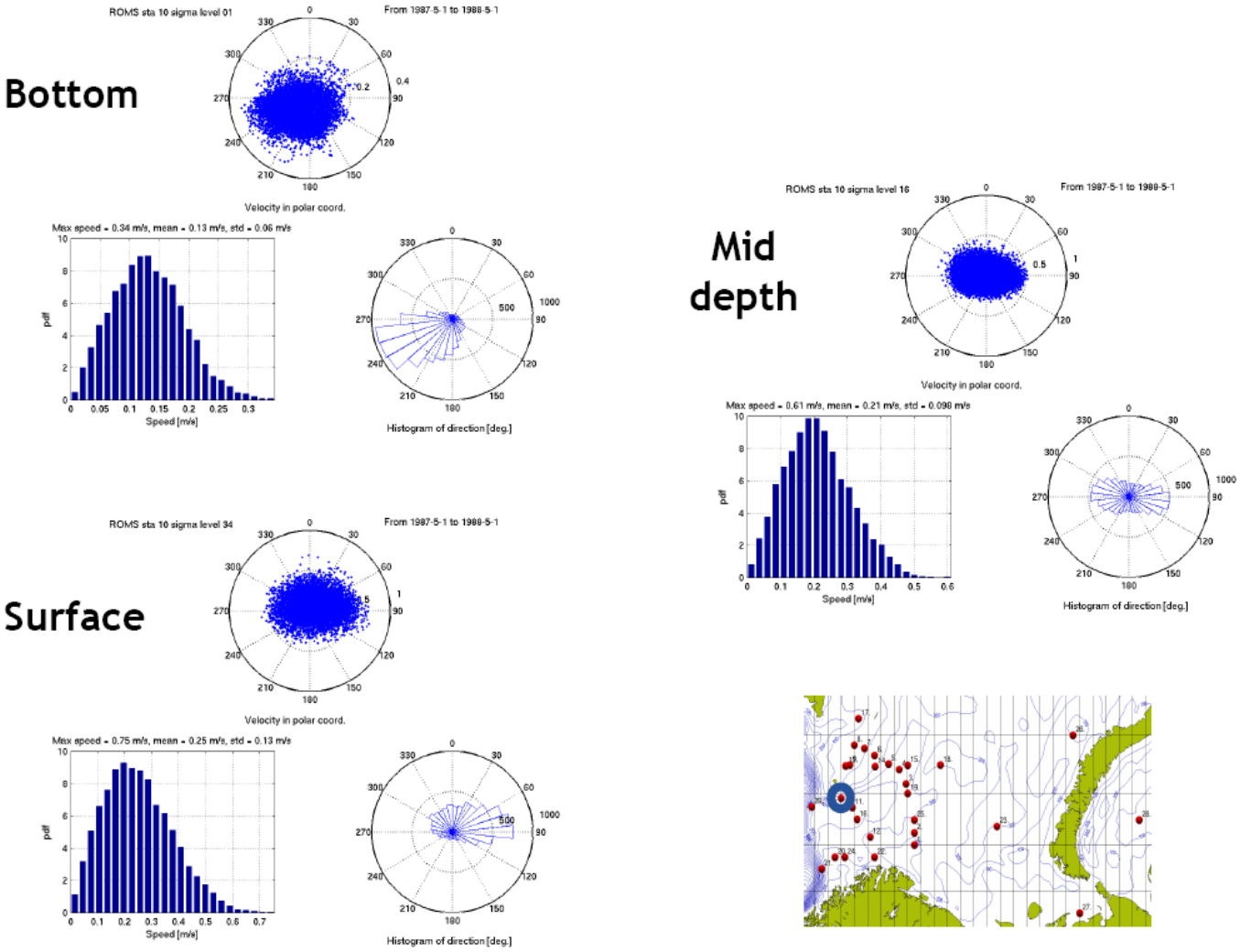

Figure 8: Current statistics based on the Phase 2 simulation from station 10 (extracted from *Røed et al.*, 2007). The location of station 10 is encircled in the lower right map. The frequency diagrams may be compared to the similar statistics from the ERA40 and HL hindcasts depicted in Figure 9, and the rotational scatter plot shown in Figure 10.

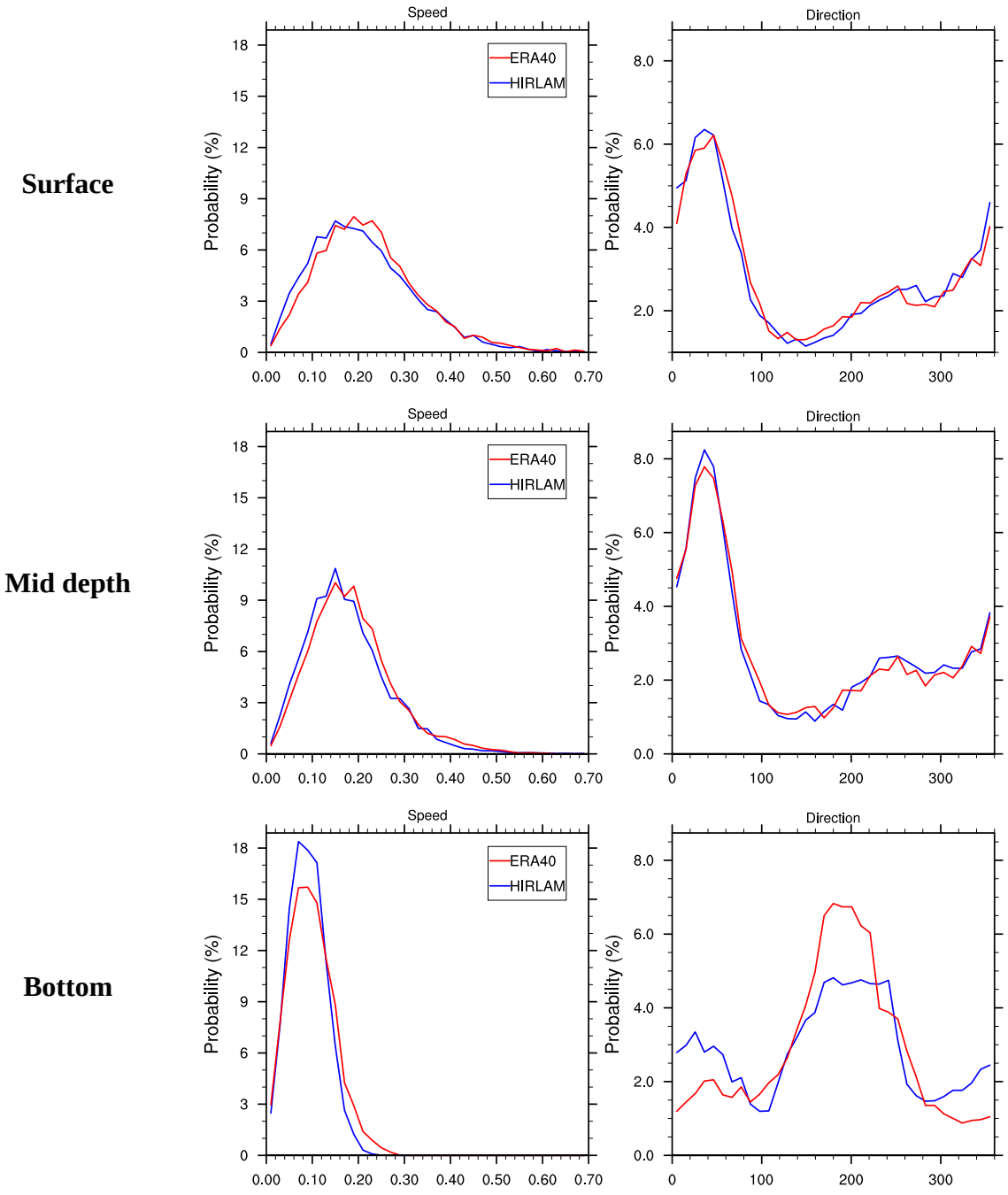

Figure 9: Displayed is the frequency diagram (PDF) at station 10 from the ERA40 (red curves) and HL (blue curves) hindcasts at the same depth levels as in Phase 2 (cf. Figure 8). Left panels show the PDFs of speed, while the right panels show the directional PDFs. Current direction from the south toward the geographical north has an angle 0, from the west toward the geographical east an angle of 90 degrees, from the north toward the geographical south an angle of 180 degrees, and from the east toward the geographical west and angle of 270 degrees.

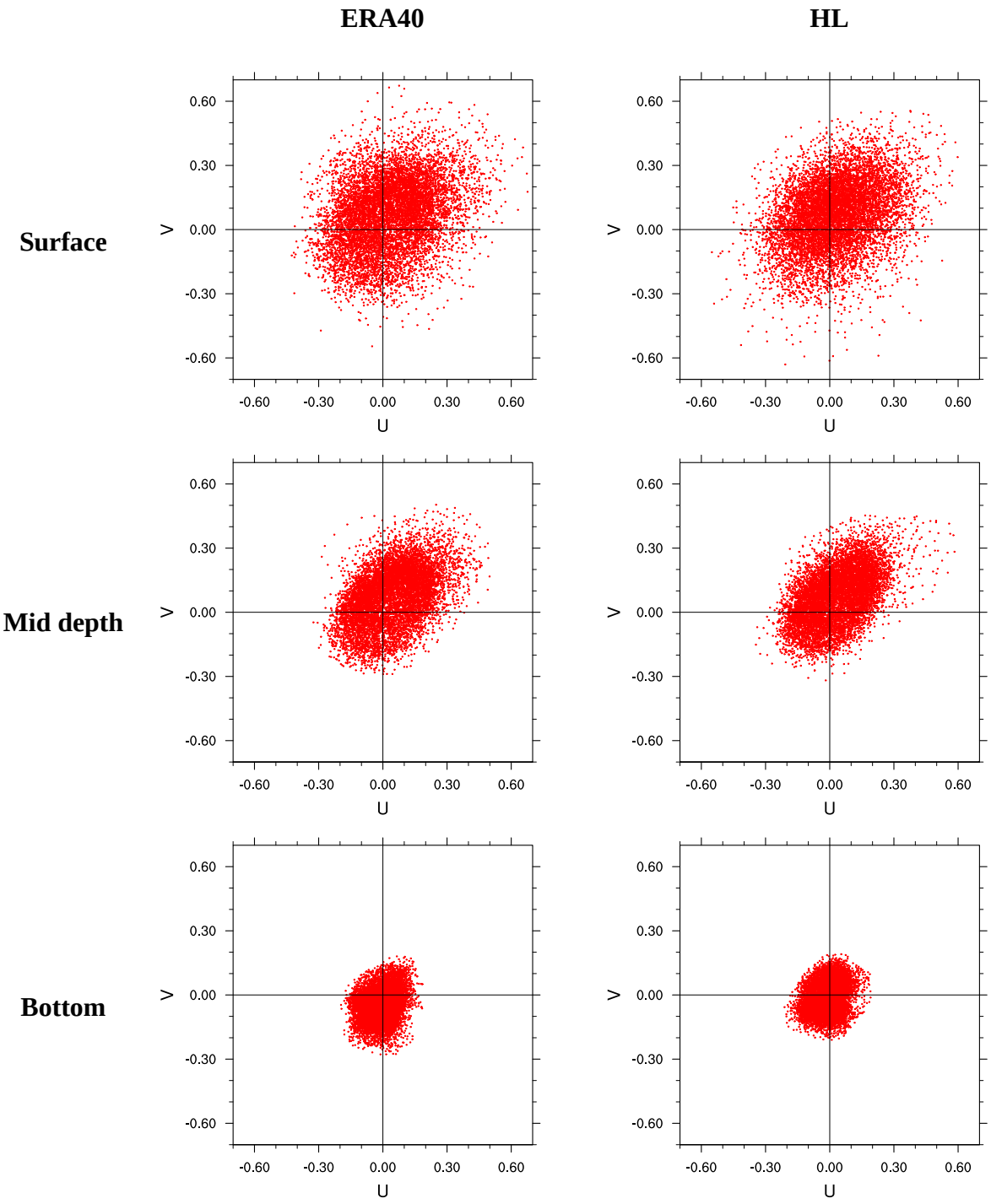

Figure 10: Displayed is the rotational scatter plot of the velocity components for station 10. Upper panels relates to the surface (sigmalevel 34), mid depth (sigmalevel 16) and bottom (sigmalevel 01), respectively. Left-hand panels show results from the ERA40 hindcasts while the right-hand panels show the results from the HL hindcast.

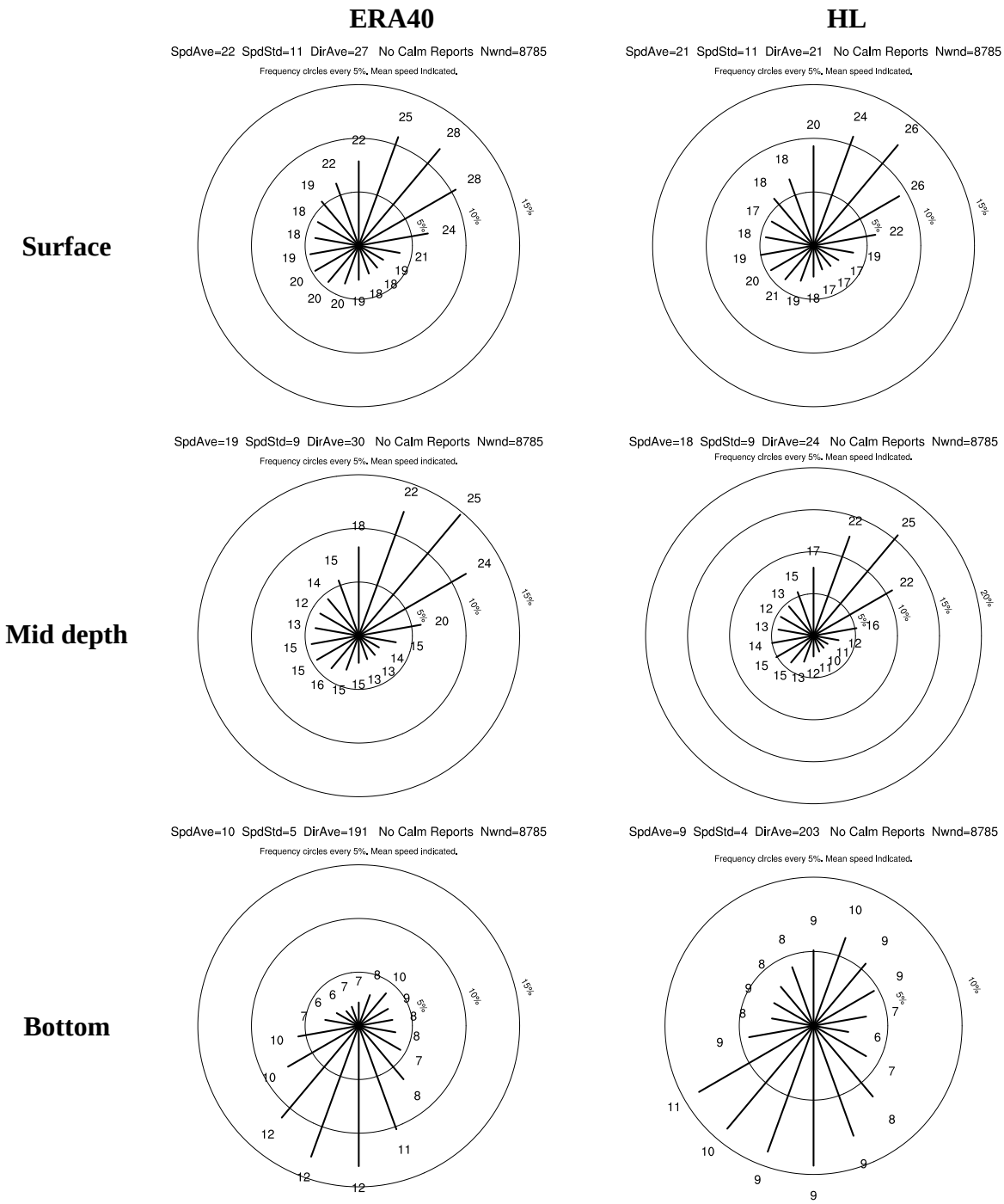

Figure 11: Displayed is the directional histogram of the velocity for station 10. Upper panels relates to the surface (sigmalevel 34), mid depth (sigmalevel 16) and bottom (sigmalevel 01), respectively. Left-hand panels show results from the ERA40 hindcasts while the right-hand panels show the results from the HL hindcast. Number attached to each direction is the mean speed in that direction in cm/s.

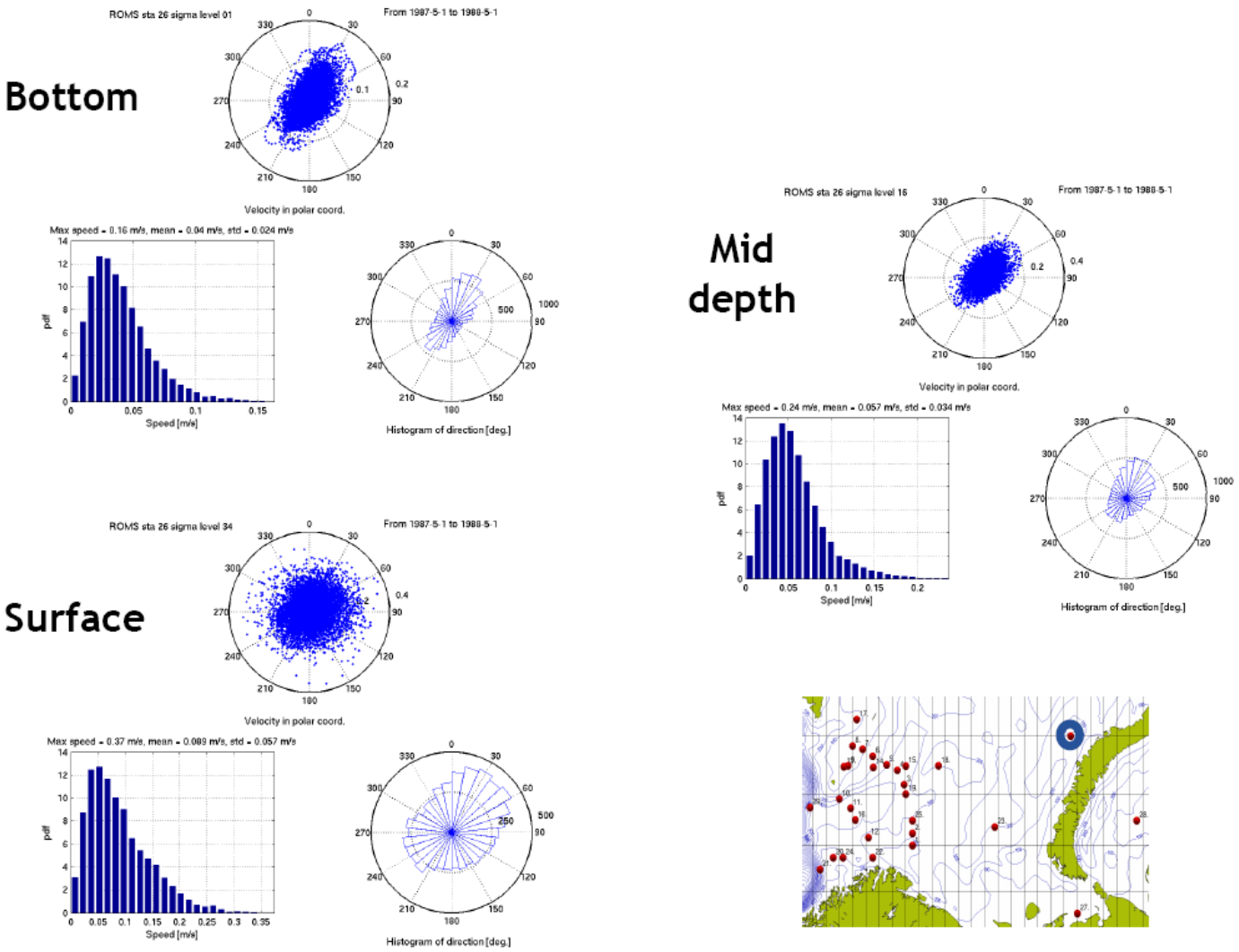

Figure 12: As Figure 8, but for station 26.

Surface

Mid depth

Bottom

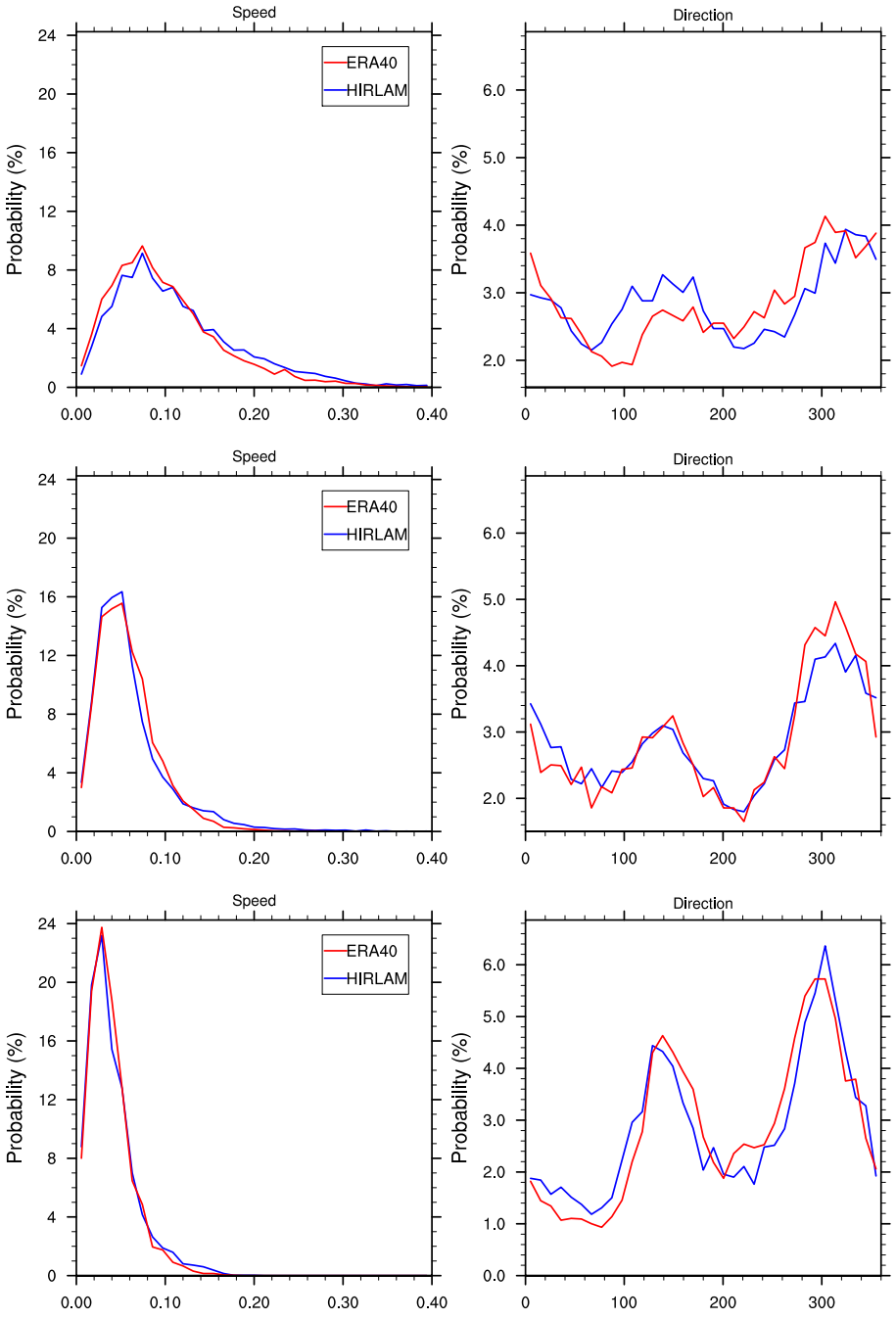

Figure 13: As Figure 9, but for station 26.

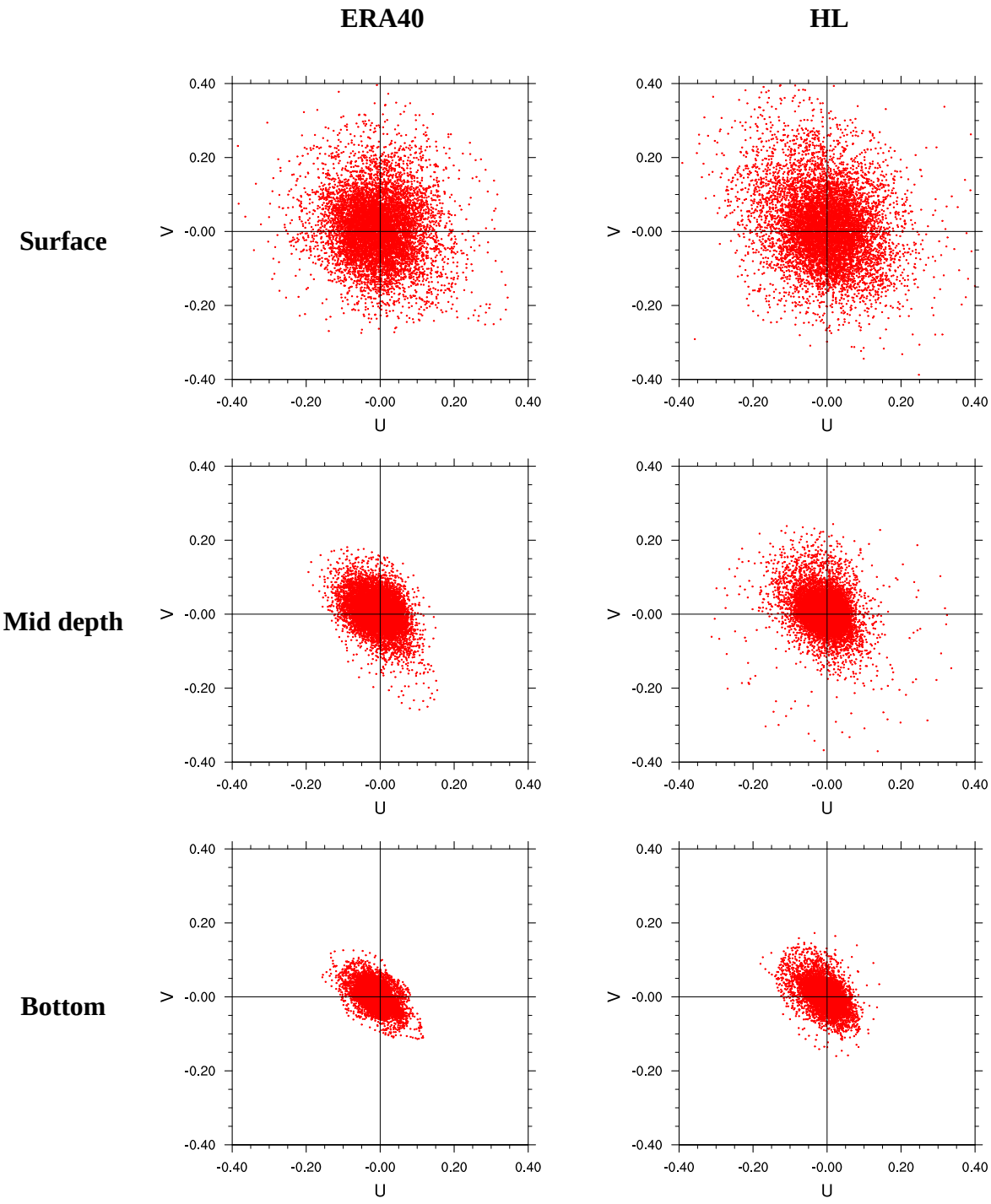

Figure 14: As Figure 10, but for station 26.

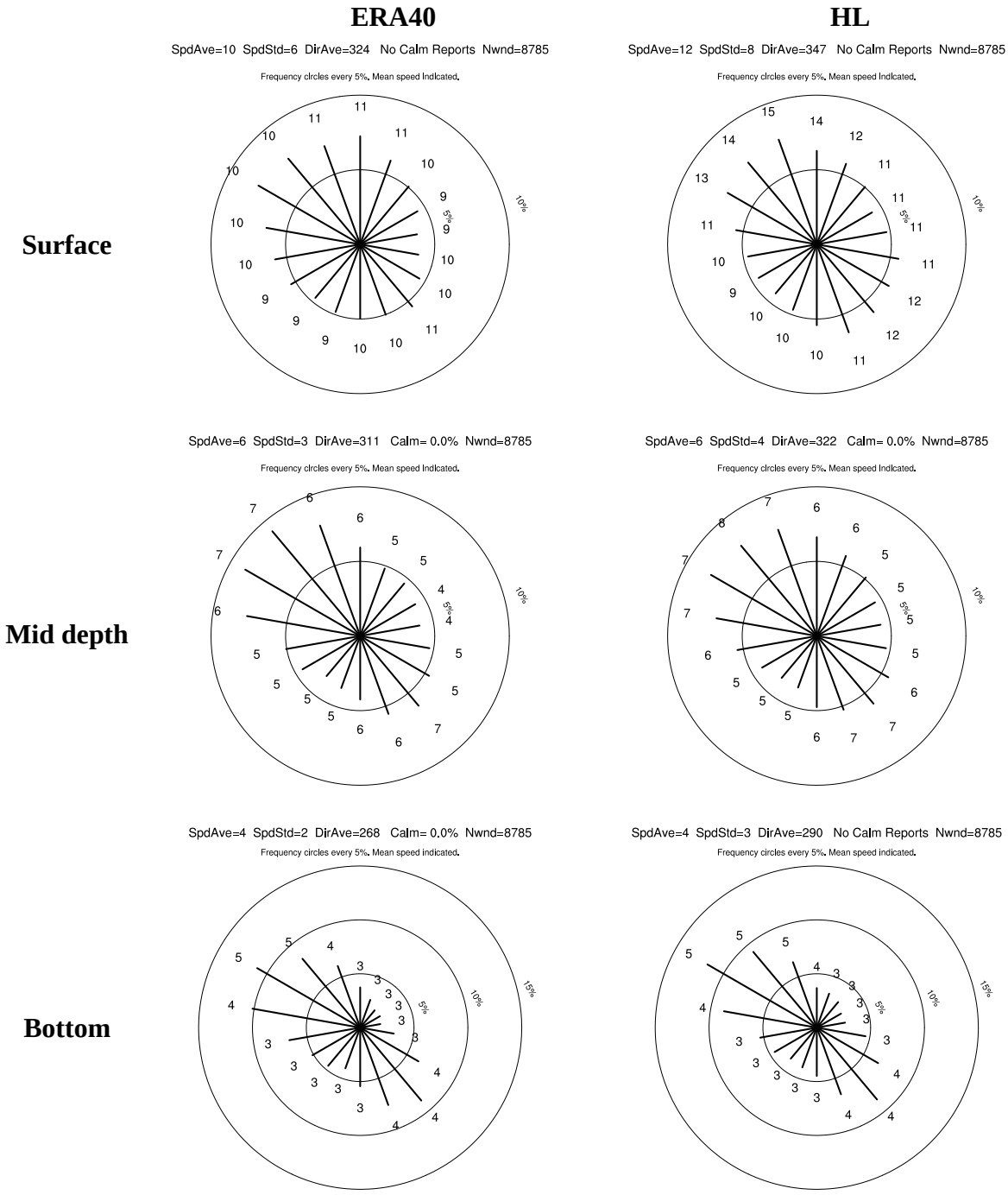

Figure 15: As Figure 11, but for station 26